



# The apple *MdGA2ox7* modulates the balance between growth and stress tolerance in an anthocyanin-dependent manner

Rui Yan<sup>a</sup>, Tianle Zhang<sup>a</sup>, Yuan Wang<sup>b</sup>, Wenxiu Wang<sup>a</sup>, Rahat Sharif<sup>c</sup>, Jiale Liu<sup>a</sup>, Qinglong Dong<sup>a</sup>, Haoan Luan<sup>a</sup>, Xuemei Zhang<sup>a</sup>, Han Li<sup>a</sup>, Suping Guo<sup>a</sup>, Guohui Qi<sup>a,\*</sup>, Peng Jia<sup>a,\*\*</sup>

<sup>a</sup> College of Forestry, Hebei Agricultural University, Baoding, 071000, China

<sup>b</sup> State Key Laboratory of North China Crop Improvement and Regulation, Hebei Agricultural University, Baoding, 071000, China

<sup>c</sup> Department of Horticulture, School of Horticulture and Landscape, Yangzhou University, Yangzhou, 225009, China

## ARTICLE INFO

### Keywords:

Anthocyanins  
Apple  
Abiotic stress  
*GA2ox7*

## ABSTRACT

Apple (*Malus domestica* Borkh.) is a widely cultivated fruit crop worldwide but often suffers from abiotic stresses such as salt and cold. Gibberellic acid (GA) plays a pivotal role in controlling plant development, environmental adaptability, and secondary metabolism. The GA2-oxidase (GA2ox) is responsible for the deactivation of bioactive GA. In this study, seventeen *GA2-oxidase* genes were identified in the apple genome, and these members could be clustered into four clades based on phylogenetic relationships and conserved domain structures. *MdGA2ox7* exhibited robust expression across various tissues, responded to cold and salt treatments, and was triggered in apple fruit peels via light-induced anthocyanin accumulation. Subcellular localization prediction and experiments confirmed that *MdGA2ox7* was located in the cytoplasm. Overexpression of *MdGA2ox7* in *Arabidopsis* caused a lower level of active GA and led to GA-deficient phenotypes, such as dwarfism and delayed flowering. *MdGA2ox7* alleviated cold and salt stress damage in both *Arabidopsis* and apple in concert with melatonin (MT). Additionally, *MdGA2ox7* enhanced anthocyanin biosynthesis in apple calli and activated genes involved in anthocyanin synthesis. These findings provide new insights into the functions of apple *GA2ox* in regulating development, stress tolerance, and secondary metabolism.

## 1. Introduction

Gibberellin (GA) is a pivotal phytohormone, exercising significant influence over the vegetative and reproductive biology of plant. Currently, 136 GAs have been identified, but only a small number of active GA forms are functionally operative (Hedden, 2020). The homeostasis of GA is regulated by a variety of enzymes, encompassing those involved in synthesis, metabolism, and transport. GA2-oxidases (GA2ox) have proven to be responsible for decreasing active GA contents in various plant species (Wuddineh et al., 2015; Tian et al., 2022). GA2ox belong to soluble 2-oxoglutarate-dependent dioxygenase, encoded by multigene families (Lange et al., 2020). The knowledge of GA2ox has progressed rapidly in recent years, largely due to the remarkable advancements in genome sequencing technologies. In *Arabidopsis thaliana*, nine members of the GA2ox family exist,

including five (AtGA2ox1 - AtGA2ox4, and AtGA2ox6) that catalyze the deactivation of C<sub>19</sub>-GAs and four (AtGA2ox7 - AtGA2ox10) responsible for the deactivation of C<sub>20</sub>-GAs (Lange et al., 2020). Tissue-specific analysis revealed that the genes are differentially expressed in various tissues during growth and development (Li et al., 2019a), indicating that GA2ox has a wide range of biological functions. The *ga2ox* quintuple and double mutant accumulated higher levels of active GAs compared to wild type (WT) plants, leading to phenotypes associated with excess GA, such as early bolting and elongated stem (Schomburg et al., 2003; Rieu et al., 2008). Conversely, overexpression of GA2ox results in a reduction of active GA content, leading to semi-dwarfism (Lo et al., 2008).

In addition to directly regulating a wide range of growth and development processes, there is increasing evidence that GA2ox is also involved in stress tolerance. β-glucuronidase (GUS) staining revealed that the majority of GA2ox genes in *Arabidopsis* were induced by various

\* Corresponding author.

\*\* Corresponding author.

E-mail addresses: [bdqgh@hebau.edu.cn](mailto:bdqgh@hebau.edu.cn) (G. Qi), [jiapeng@hebau.edu.cn](mailto:jiapeng@hebau.edu.cn) (P. Jia).

<https://doi.org/10.1016/j.plaphy.2024.108707>

Received 11 January 2024; Received in revised form 19 April 2024; Accepted 5 May 2024

Available online 8 May 2024

0981-9428/© 2024 Published by Elsevier Masson SAS.

stress treatments (Li et al., 2019a). In Arabidopsis, *AtGA2ox9* contributes to freezing tolerance (Lange et al., 2020) and *AtGA2ox7* confers resistance to high-salinity stress (Magome et al., 2008). In addition to the semi-dwarf, overexpression of *PvGA2ox5* and *PvGA2ox9* from switchgrass (*Panicum virgatum* L.) resulted in characteristic GA-deficient phenotypes with dark-green leaves (Wuddineh et al., 2015). Thus, it seems that the decreased active GA content under stress conditions, via the up-regulated expression of *GA2ox*, is beneficial for plant to adapt to adverse environments. Moreover, melatonin (*N*-acetyl-5-methoxytryptamine, MT), another new emerging plant hormone, plays an increasingly prominent role in plant stress (Sun et al., 2021). Various studies have demonstrated that MT plays a more prominent role in plant development, particularly in enhancing plant tolerance to unfavorable environmental conditions. For example, molecular and physiological evidence has supported the involvement of both MT exogenous application and endogenous MT content in enhancing salinity tolerance in Arabidopsis (Hernández et al., 2015; Su et al., 2021). Reactive oxygen species (ROS), a by-product of aerobic metabolism, serve as crucial signaling molecules in stress responses (Zaid and Wani, 2019). MT has been shown to up-regulate the expression of transcription activators related to ROS-scavenging antioxidant genes, thereby alleviating cold stress response (Bajwa et al., 2014). Additionally, MT emerges as a multi-functional regulatory molecule that interacts with the activities of other phytohormones. For instance, MT induces parthenocarp by promoting GA biosynthesis in pear (*Pyrus communis* L.) and inhibits seed germination by crosstalk with GA in Arabidopsis (Liu et al., 2018; Lv et al., 2021). Moreover, GA plays a pivotal role in secondary metabolism. Notably, exogenous application of GA has been found to suppress anthocyanin accumulation by downregulating the expression of genes involved in anthocyanin synthesis (An et al., 2023). Components of the GA signaling pathway are also involved in modulating anthocyanin content (Xie et al., 2016).

In the modern apple industry, an increasing demand for controlled tree size offers numerous horticultural benefits, such as reduced stature for high-density cultivation, intensive management, and reasonable flowering time and number of flowers (Wang et al., 2019). Furthermore, given the escalating salinity levels in soil and the disruptive effects of extremely low temperatures, salt, and cold tolerance have emerged as critical considerations in apple breeding programs. The regulation of GA metabolism plays a pivotal role in modulating these horticultural traits. However, our understanding of GA metabolism-related genes and their functional roles remains incomplete. Consequently, we embarked on a study to delve deeper into the *GA2ox* genes in apple and specifically investigate the role of *MdGA2ox7* in regulating growth, development, stress response, and anthocyanin accumulation. Our findings will offer valuable insights and present an ideal candidate gene for molecular breeding to create apples with diverse and exceptional horticultural traits.

## 2. Materials and methods

### 2.1. Plant materials and treatments

Apple 'GL3' tissue culture seedlings were subcultured in MS medium supplemented with IBA ( $0.2 \text{ mg L}^{-1}$ ) and 6-BA ( $0.3 \text{ mg L}^{-1}$ ). For cold treatment, the shoots were subjected to freezing at  $-2^\circ\text{C}$  for 1 h, subsequently cultured in an incubator maintained at  $4^\circ\text{C}$ . For salt treatment, NaCl was added to the medium at a final concentration of  $150 \text{ mmol L}^{-1}$ . To detect the relief effect of MT on stress damage, MT was added to the medium at a final concentration of  $0.2 \text{ } \mu\text{mol L}^{-1}$ .

Arabidopsis (Columbia ecotype, Col-0), tobacco (*Nicotiana tabacum* L.), and the 'Orin' apple calli were cultivated as previously described (Jia et al., 2021). For short-term stress treatment of Arabidopsis and tobacco, seedlings were exposed to  $4^\circ\text{C}$  for 3 h or soaked in  $150 \text{ mmol L}^{-1}$  NaCl solution for 1 day. For long-term stress treatment, Arabidopsis seedlings underwent cold acclimation at  $4^\circ\text{C}$  for 1 d, followed by

exposure to  $-8^\circ\text{C}$  for 5 h. Subsequently, they were allowed to recover at  $4^\circ\text{C}$  for 12 h and then grown at  $23^\circ\text{C}$  for 5 days, during which the survival rate was calculated. Additionally, seedlings were also grown on MS plates containing  $150 \text{ mmol L}^{-1}$  NaCl to detect salt stress tolerance, and the green cotyledon ratios were counted at 12 d after seed imbibition.

The apple calli were grown on MS medium maintained at  $4^\circ\text{C}$ , or on MS supplemented with NaCl ( $150 \text{ mmol L}^{-1}$ ) for half a month for cold and salt treatments, respectively.

### 2.2. Genome-wide identification of the *GA2-oxidase* genes

To identify the *GA2-oxidase* protein encoded by the apple genome, a homology-based comparison was performed. Using the protein sequences of nine *AtGA2ox* in Arabidopsis as queries, the BLAST (Basic Local Alignment Search Tool) algorithm was employed to search for a protein dataset from apple with an expected value threshold of  $1\text{E-}5$ . The retrieved protein sequences were subsequently analyzed in the Pfam and the NCBI CCD database. After manually removing the redundancy, candidate genes were named according to their chromosomal location. ExPASy was employed to analyze the *GA2ox* protein's physical and chemical properties. Subcellular locations were predicted by the Plant-mPLOC online website (<http://www.csbio.sjtu.edu.cn/bioinf/pla-nt-multi/>).

### 2.3. Phylogenetic tree, gene structure, and conserved domains analysis

The phylogenetic tree comparing *GA2ox* proteins from Arabidopsis and apple was produced by the MEGA7.0 software with the following parameters: JTT + G model with a bootstrap of 1000 replications. The introns, exons, and untranslated regions of each member are visualized using GSDS software, based on gene structure files. Conserved domains within *GA2ox* proteins were elucidated with the MEME platform (<https://meme-suite.org/meme/>).

### 2.4. Chromosome location, synteny, and promoter sequence analysis

The chromosomal location of the *MdGA2ox* genes was visualized using the TB tool software, according to the gene structure gff3 file. The OrthoMCL was adopted to search the paralogous *GA2ox* within the apple genome as well as between apple and Arabidopsis genomes, to examine the association between collinearity and duplication events. The 1500-bp sequence (promoter) upstream of the start codon 'ATG' was analyzed using PlantCARE (<https://bioinformatics.psb.ugent.be/webtools/plantcare/html/>) to determine the *cis*-regulatory element (CRE). The diversity of CRE was subsequently categorized and visualized.

### 2.5. Temporal and spatial expression analysis

Spatial expression features of *MdGA2ox* were obtained by analyzing the Gene Expression Omnibus (GEO) database from 16 apple tissues under accession number GSE42873. The gene expression profiles of *MdGA2ox* at the crucial time of floral transition were obtained by searching the transcriptome data reported previously (Li et al., 2019b). The transcriptome data of apple peel samples at different time points in the process of changing from green to red under light conditions after unbagging was downloaded in the GEO database under accession number GSE185089.

### 2.6. Gene cloning, vector construction, and plant transformation

The cloning of the promoter and coding sequence (CDS) were performed as described previously (Jia et al., 2023), using the genomic DNA and cDNA from flower buds as templates, respectively. To visualize the expression pattern of *MdGAox7*, a GUS reporter vector driven by the *MdGAox7* promoter was constructed as a previous description (Jia et al., 2023). The *MdGAox7* CDS was inserted into the pC3301-EGFP and

**Table 1**

Characterization of *MdGA2ox* gene family members.

Name	Gene ID	Location (start)	Location (end)	Strand	Length	CDS (bp)	Peptide (aa)	pI	MW (Da)
MdGA2ox1	MD03G1066600	5,313,590	5,315,802	–	2212	1086	361	5.42	40335.87
MdGA2ox2	MD03G1210700	28,974,217	28,979,233	+	5016	804	267	5.75	30354.47
MdGA2ox3	MD05G1207000	33,633,795	33,636,315	+	2520	1014	337	5.77	37427.46
MdGA2ox4	MD05G1283800	41,773,566	41,775,201	–	1635	1029	342	6.61	37871.62
MdGA2ox5	MD05G1341000	46,166,830	46,174,626	+	7796	1161	386	6.35	44028.55
MdGA2ox6	MD09G1286800	36,564,698	36,566,828	+	2130	708	235	8.18	26825.77
MdGA2ox7	MD10G1194100	29,020,103	29,022,348	+	2245	1014	337	6.2	37680.84
MdGA2ox8	MD10G1262000	35,639,451	35,641,331	–	1880	1029	342	6.72	38052.69
MdGA2ox9	MD10G1314500	39,874,287	39,877,183	+	2896	1029	342	6.72	39029.48
MdGA2ox10	MD11G1071600	6,098,728	6,100,787	–	2059	1089	362	5.59	40263.67
MdGA2ox11	MD11G1225300	32,965,225	32,965,710	+	485	486	161	6.29	18937.73
MdGA2ox12	MD11G1225400	32,971,450	32,972,701	+	1251	531	176	6.3	19954.84
MdGA2ox13	MD13G1008700	535,651	537,084	–	1433	1008	335	5.59	37758.67
MdGA2ox14	MD13G1148400	11,634,222	11,639,701	–	5479	1041	346	6.26	38457.65
MdGA2ox15	MD16G1006700	508,884	510,765	–	1881	1008	335	5.94	37783.94
MdGA2ox16	MD16G1148400	11,637,617	11,640,226	–	2609	795	264	4.86	28759.54
MdGA2ox17	MD17G1279100	33,892,030	33,896,236	+	4206	1080	359	7.56	40059.6

pC2300-EGFP vectors for overexpression, conferring resistance to basta and kanamycin, respectively. Additionally, the antisense vector *MdGA2ox7-Anti*, was also prepared to suppress the *MdGAox7* expression. Plant transformation for apple calli and Arabidopsis was carried out with the *Agrobacterium* infection method (An et al., 2023).

## 2.7. GUS staining and GFP observation

Transient *GUS* expression in tobacco leaf was determined by staining and *GUS* activity detection as described previously (Jia et al., 2023). The *GUS* expression in transgenic Arabidopsis was also detected by staining as described previously (Jia et al., 2021). Subcellular localization of *MdGA2ox7* was carried out through observation of the green fluorescent protein (GFP) signal produced by *35S::MdGA2ox7-EGFP* expression cassette. The concrete operation was described concerning our previous article (Jia et al., 2021).

## 2.8. Histochemical staining and physiological measurement

The Superoxide anion  $O_2^-$  accumulation was visualized by histochemical staining with nitroblue tetrazolium (NBT), and its level was quantified by spectrophotometric method (Yang et al., 2020). To detect the degree of photosystem damage caused by stress, chlorophyll fluorescence transients were examined in leaves from whole plants using the PlantExplorer (PhenoVation, Holland) instrument, and *Fv/Fm* ratios were calculated.

The endogenous active GA content was quantified by the ESI-HPLC-MS/MS method and performed by the AGLIENT1260 high-performance liquid chromatography in tandem with the 6420A mass spectrometry. Briefly, samples were ground into powder in liquid nitrogen, and acetonitrile extraction buffer was added and shaken at 4 °C overnight. After centrifuging at 12000 g for 5 min, the supernatant was transferred to a fresh tube containing C18 filler for further extraction. The crude extract was then blow-dried with nitrogen, redissolved with methanol, and filtered through 0.22 μm organic phase membrane, ready for HPLC-MS/MS for detection. The liquid chromatography conditions were set as follows: Chromatographic column, poroshell 120 SB-C18 reverse-phase column (2.1 × 150, 2.7 μm); Column temperature, 30 °C; Mobile phase, 0.1% formic acid-methanol with gradient elution. Mass spectrum parameters were set as follows: Ionization mode, ESI positive and negative ion mode respectively; Scan type, MRM; Air curtain gas, 15 psi; Spray voltage, +4500 V, –4000 V; Atomizing gas pressure, 65 psi; Auxiliary gas pressure, 70 psi; Atomization temperature, 400 °C.

## 2.9. Anthocyanin measurement

Apple callus was immersed in a hydrochloric acid-methanol solution and extracted in the dark at 4 °C overnight. Subsequently, the anthocyanin extract was obtained through centrifugation at 4 °C at 12,000 rpm for 15 min. The absorbance of the anthocyanin extract was then measured at 530, 620, and 650 nm using a spectrophotometer (UV 8000S, METASH, Shanghai, China). Anthocyanin content was calculated using the formula  $(A_{530} - A_{620}) - (0.1 \times (A_{650} - A_{620}))$ .

## 2.10. Real-time quantitative PCR (qRT-PCR) analysis

Total RNAs were extracted from plant materials and subjected to reverse transcription with an RT Reagent Kit (Tiangen, China). qRT-PCR was performed using a TransStart® Green qPCR SuperMix (TransGen Biotech, China). Primers used for gene expression analysis are listed in Table S2.

## 2.11. Statistical analysis

Experimental data was analyzed using the SPSS software and presented as the mean ± SD. Asterisks (\*) or different letters indicated the significant difference assessed by the Student's *t*-test ( $p < 0.05$ ).

# 3. Results

## 3.1. Genome-wide identification of the GA2-oxidase in apple

Nine GA2-oxidase coding genes in *A. thaliana* have been identified: these are AtGA2ox1–4, 6–10 (AtGA2ox5 was omitted due to its pseudogene status). The nine AtGA2ox protein sequences were utilized as a query and through the Blastp algorithm, we retrieved the GA2ox genes in apple GDDH13 genome data (<https://iris.angers.inra.fr/gddh13/>). Following manual verification and redundancy reduction, the 17 GA2ox members were obtained and given the names MdGA2ox1 to MdGA2ox17 (Table 1).

## 3.2. Phylogenetic tree of GA2-oxidase genes

The neighbor-joining tree constructed comparing the GA2ox from apple and *A. thaliana* (Fig. 1A) revealed that the GA2ox proteins can be categorized into four distinct groups, labeled Group I, II III, and IV. Group I and II were further designated as C<sub>19</sub>-GA2ox-I and C<sub>19</sub>-GA2ox-II, respectively. The Group I encompassed two GA2ox from *A. thaliana* (AtGA2ox4, AtGA2ox6) and five from apple. The group II contained three AtGA2ox (AtGA2ox1–3) and four MdGA2ox (MdGA2ox3–4,

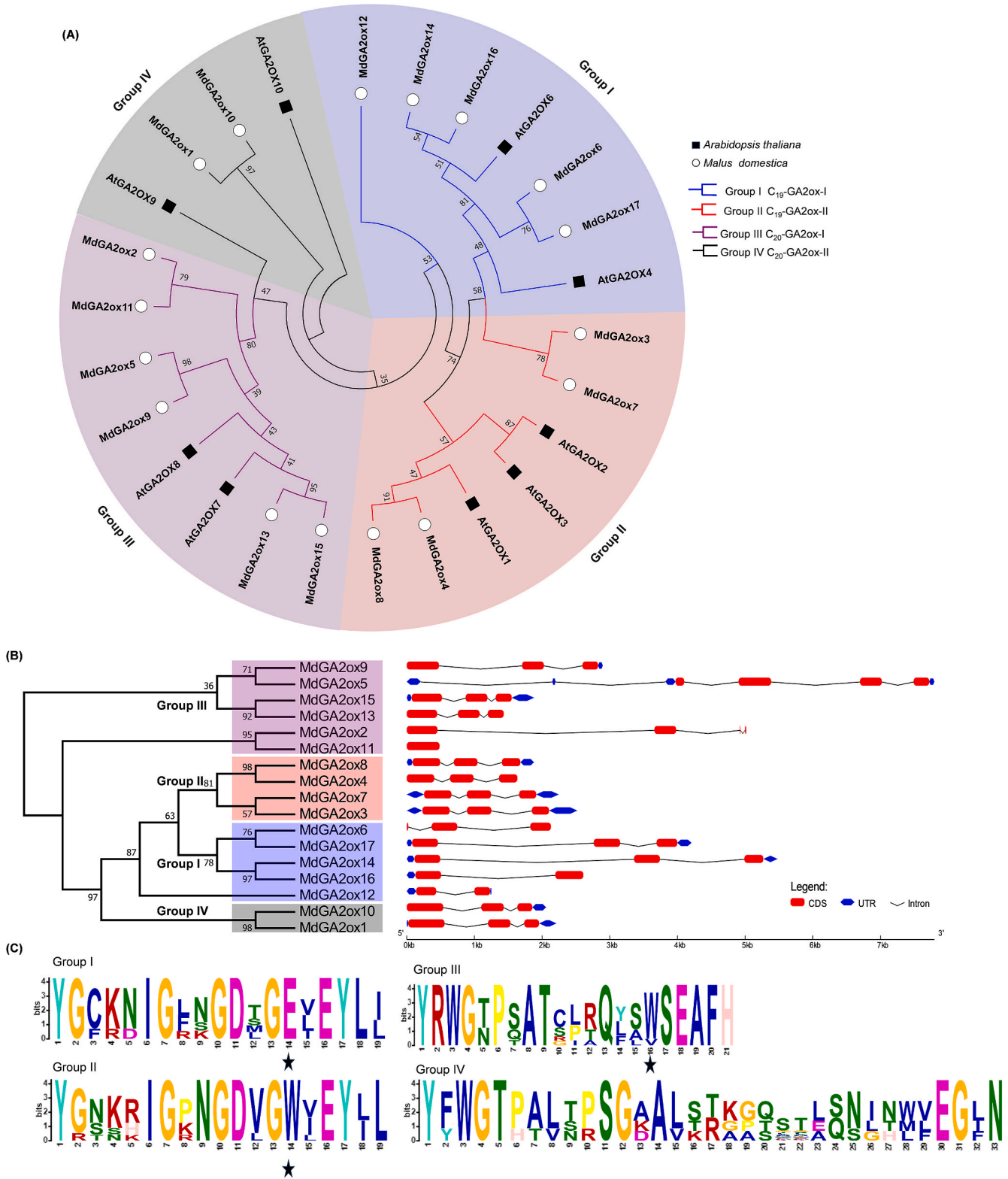


**Fig. 1.** Phylogenetic tree, Gene structure, and conservative motif analysis of the GA2-oxidase gene family members. (A) A neighbor-joining tree representing phylogenetic relationships, based on the Jones-Taylor-Thornton (JTT) matrix-based model and gamma (G) distribution. Different shadows indicate different subgroups. Bootstrap analysis with 500 replications was performed to assess the reliability of the phylogenetic topology. (B) **Gene structure analysis.** The gene structure map was shown with the GSDS online analysis tool. The phylogenetic tree shown on the left panel was constructed with the JTT + G method. Different shadows indicate different subgroups. (C) **Conservative motif prediction.** The conservative motif showed the amino acid sequence feature in the N-terminal of different GA2-oxidase groups. Asterisks highlight differences in conserved amino acids.

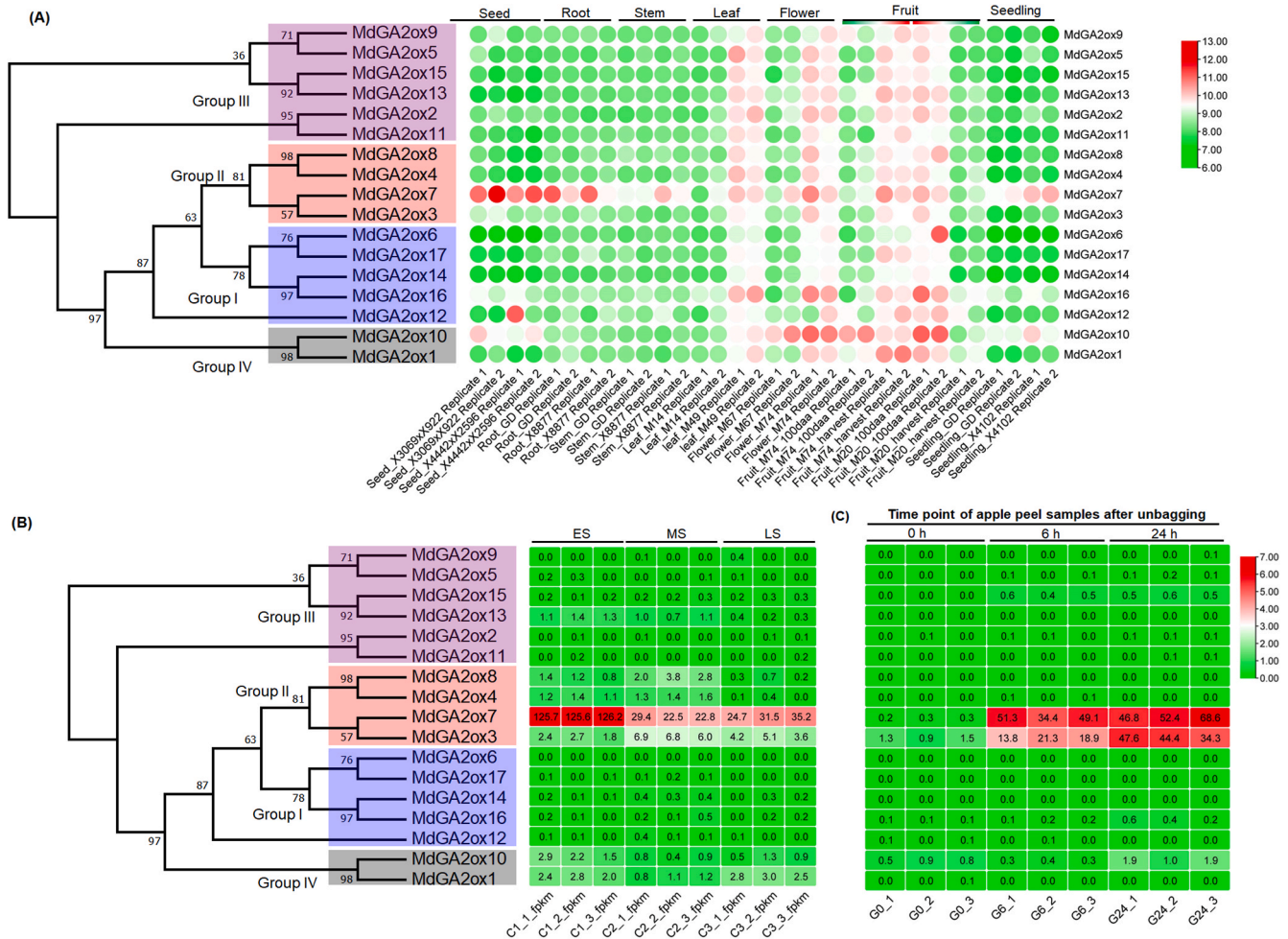


**Fig. 2.** Temporal and spatial expression characteristics of MdGA2ox family genes. (A) MdGA2ox gene expression profiles in different tissues. (B) Expression dynamics of MdGA2ox genes during flowering induction. (C) Expression patterns of MdGA2ox genes in apple peels undergoing a color transition from green to red under light conditions after unbagging. For (B) and (C), the color and value of the different blocks indicate the level of expression.

MdGA2ox7 -8). These findings suggest that these nine apple MdGA2ox enzymes can utilize C<sub>19</sub>-GAs as substrates (Rieu et al., 2008). Two AtGA2ox (AtGA2ox7 -8) and six MdGA2ox clustered into the Group III three, also known as group C<sub>20</sub>-GA2ox-I. These enzymes are likely to be primarily active against C<sub>20</sub>-GAs. The group IV included two AtGA2ox (AtGA2ox9 -10) and two MdGA2ox (MdGA2ox1 and MdGA2ox10), which might also act on GA precursors containing a C<sub>20</sub>-skeleton (Lange et al., 2020).

### 3.3. Apple GA2-oxidase gene structure and conserved motif

The gene structure pattern analysis revealed (Fig. 1B) that MdGA2ox genes typically contained two to three introns, with a relatively consistent exon-intron organization among the different groups. Specifically, all members of group II exhibited a conserved structure with two introns and three exons. However, MdGA2ox2 and MdGA2ox11 differed in the number and arrangement of introns and exons despite their close genetic relationship. Such differences in gene structure suggest that MdGA2ox2 and MdGA2ox11 may have undergone functional divergence during evolution.

The molecular weight of MdGA2ox proteins ranged significantly, varying from a low of 18.94 kDa (MdGA2ox11) to a high of 44.03 kDa (MdGA2ox5) (Table 1). The analysis of the amino acid sequence signature within the N-terminus of MdGA2ox proteins revealed notable similarities and differences among the different groups. The group I (C<sub>19</sub>-GA2ox-I) and group II (C<sub>19</sub>-GA2ox-II) shared highly conserved

amino acids except for the fourteenth amino acid (Glutamic/E in group I while Tryptophan/W in group II). Meanwhile, the sequence identity among the members of group III was comparatively low. Nevertheless, there is a relatively conserved W in the sixteenth position of the motif (corresponding to the 14th position of group I and II). This conserved residue suggests that group II occupies a transitional position between group I and group III in terms of sequence similarity. In contrast, the N-terminal motif of group IV members displayed greater variability compared to group III (Fig. 1C).

### 3.4. Chromosome distribution and collinearity analysis

The seventeen MdGA2ox genes exhibited a non-uniform distribution across eight chromosomes. Specifically, chromosomes 05, 10, and 11 each harbored three MdGA2ox genes, while chromosomes 03, 13, and 16 each contained two. Chromosomes 09 and 17 each hosted a single MdGA2ox gene (Supplementary Fig. S1A). To gain insights into the gene expansion process within this family, we delved into the MdGA2ox gene duplication events. Notably, a total of 13 gene pairs were identified in duplicate regions of the apple genome (Supplementary Fig. S1A). Five pairs of syntenic orthologous genes were matched between apple and Arabidopsis (Supplementary Fig. S1B).

### 3.5. Cis-regulatory elements in apple GA2-oxidase promoter

Cis-regulatory elements (CREs) in the MdGA2ox promoter region

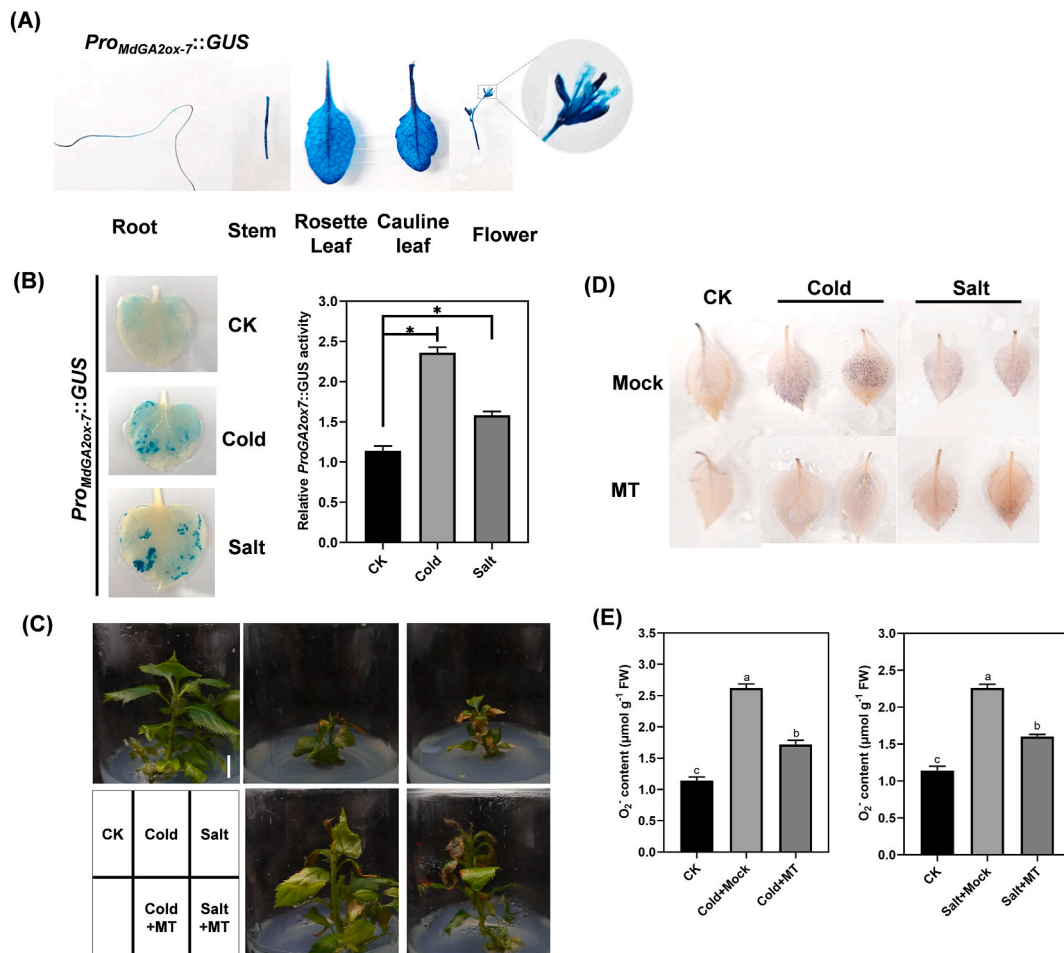


**Fig. 3.** The expression pattern of *MdGA2ox7* and the alleviative effect of MT on the injury of apples to cold and salt stress. (A) GUS staining showed the promoter activity of *MdGA2ox7* in different Arabidopsis tissues. (B) GUS staining and activity measurement showed the response of *MdGA2ox7* promoter activity to cold and salt stress. (C) Phenotypic comparison of apple seedlings with and without MT supplementation under cold and salt stress. (D)–(E) Detection of reactive oxygen species (ROS) under different stress conditions. (D) Nitro Blue Tetrazolium (NBT) staining showed the accumulation of superoxide anion radical in apple leaves under different stress and MT applications. (E) The content of superoxide anion radical in apple leaves. Bar = 1 cm.

were analyzed to explore their possible involvement in developmental regulation and environmental cue response (Supplementary Fig. S2). Certain CREs relevant to developmental regulation and tissue-specific expression, like circadian control, endosperm expression, meristem expression, cell cycle regulation, and seed-specific regulation, were expected. The promoter of *MdGA2ox* genes also contains environmental and stress-related CREs, such as light responsiveness, anaerobic induction, low-temperature responsiveness, drought-inducibility, and defense and stress responsiveness. Furthermore, it is anticipated that several hormone-responsive elements such as gibberellin, auxin, salicylic acid, MeJA, and abscisic acid are present in the promoters of numerous *MdGA2ox* members. Collectively, these findings suggest that the *MdGA2ox* gene family may play a role in various aspects of plant growth and development.

### 3.6. Expression profiles of apple GA2-oxidase genes and the subcellular localization

The specificity of gene function can be inferred through tissue expression profiles. Leveraging GEO data encompassing sixteen different tissues, we delineated the transcription pattern of the *MdGA2ox* genes (Fig. 2A). Notably, the majority of *GA2ox* genes exhibited preferential expression in reproductive organs, such as flowers and fruits, with group IV members standing out prominently. Intriguingly, during the growth of two distinct fruit types (M74 and M20), the

expression pattern of *MdGA2ox* exhibited an inverse trend from 100 days after anthesis to harvest. Conversely, the expression in vegetative organs is generally at a low level. Significant disparities were observed in the expression of *MdGA2ox* in the leaves of the two cultivars, M14 and M49. Notably, *MdGA2ox7*, belonging to group II, displayed robust transcription levels across all detected tissues.

Floral induction is the crucial precursor to apple flowering. Thus, the expression patterns of the *MdGA2ox* gene family were characterized during the process of floral induction (Fig. 2B). Notably, *MdGA2ox7* had the highest transcript abundance in flower buds throughout the physiological differentiation period compared to all other members, indicating its pivotal in regulating flower transition. Furthermore, the transcriptional level of *MdGA2ox7* was down-regulated as flower bud differentiation progressed. In addition, only *MdGA2ox7* and *MdGA2ox3* exhibited robust expression in apple peel samples, and were activated in the process of changing from green to red under light conditions after unbagging (Fig. 2C). These findings underscore the intricate role of *MdGA2ox* genes, particularly *MdGA2ox7*, in apple development and coloration.

### 3.7. *MdGA2ox7* expression is activated in response to salt and cold stress

The *MdGA2ox7* promoter exhibited activity across all plant tissues, including reproductive organs like flowers and vegetative organs like roots, stems, and leaves, as demonstrated by GUS staining (Fig. 3A).

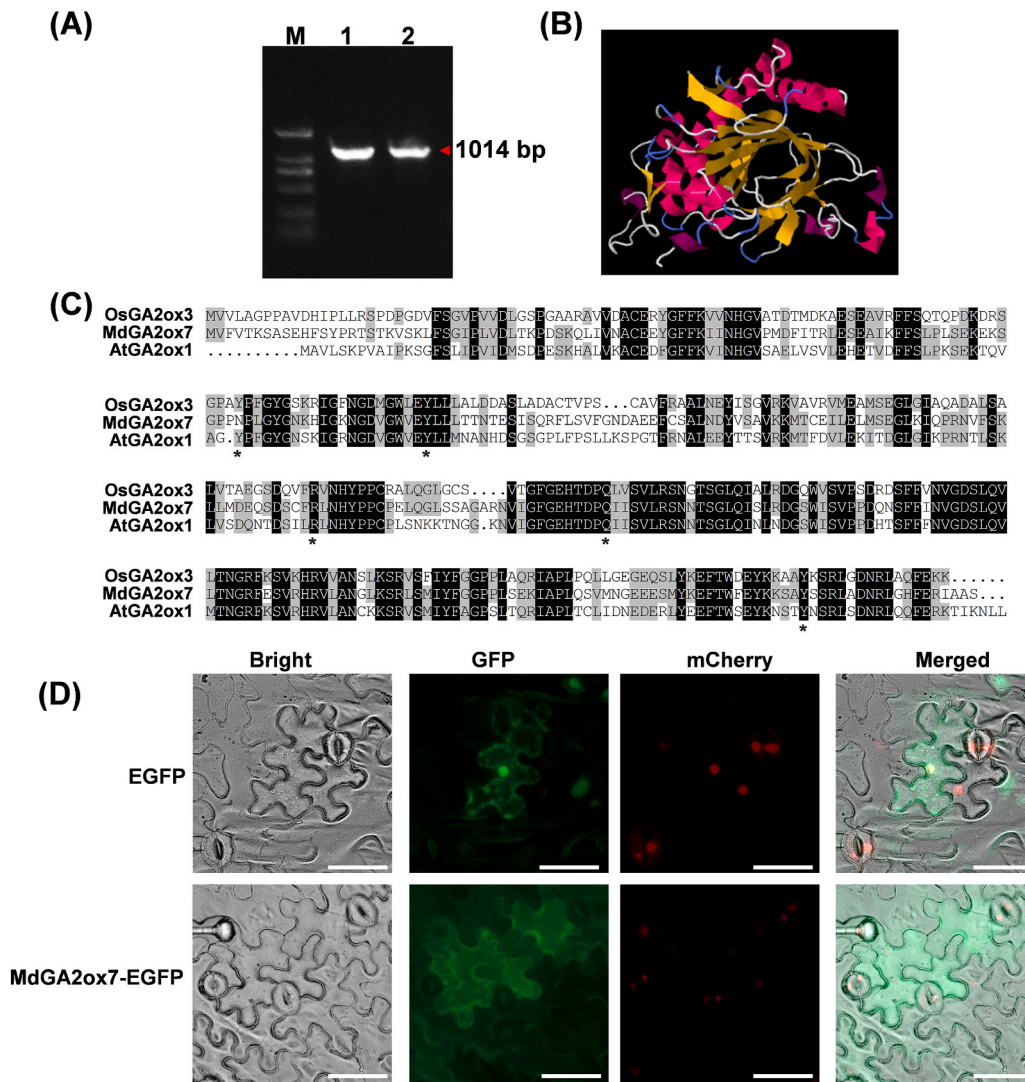


**Fig. 4.** Gene cloning, protein structure, and subcellular localization of *MdGA2ox7*. (A) PCR amplification of the *MdGA2ox7* coding sequence. Lane M, DNA molecular weight marker. The red arrow indicates the target band. (B) Three-dimensional structure prediction of *MdGA2ox7* protein. The crystal structure of *MdGA2ox7* is based on the reported *OsGA2ox3* data, with a confidence of 100.0% and a coverage of 93%.  $\alpha$ -helices and  $\beta$ -strands are shown in different colors. (C) Multiple sequence alignment analysis of *MdGA2ox7* and two GA2ox from Arabidopsis (*AtGA2ox1*) and rice (*OsGA2ox3*). Amino acids interacting with GA<sub>4</sub> (Q206, Y312, Y89, Y109, and R179) are indicated with asterisk. (D) Subcellular localization of *MdGA2ox7*. The 35S::MdGA2ox7-EGFP and the control 35S::EGFP expression cassette were transiently expressed in tobacco leaves and visualized using a confocal microscope. The NLS-mcherry indicates the nucleus. Scale bar, 10 μm.

Furthermore, its promoter activity was triggered by abiotic stress such as cold and salt treatments (Fig. 3B). These two abiotic stresses can directly hinder apple growth, and the results of NBT staining and superoxide anion measurements revealed a surge in reactive oxygen species (ROS) (Fig. 3C–E). Additionally, the supplementation of MT significantly alleviated the growth inhibition and ROS accumulation caused by cold and salt stress (Fig. 3C–E). It is suggested that *MdGA2ox7* and MT play an interactive role in regulating apple stress response.

The encoding sequence of *MdGA2ox7*, spanning 1014 base pairs, was isolated (Fig. 4A).  $\alpha$ -helices,  $\beta$ -strands, and random coils were embedded in the three-dimensional structure of *MdGA2ox7*, predicted according to the structure of *OsGA2ox3* (Takehara et al., 2020) (Fig. 4B). Multiple sequence comparisons demonstrated a high degree of conservation in the amino acids responsible for interacting with GA<sub>4</sub> within GA2ox across various species (Fig. 4C). Subcellular localization results revealed that *MdGA2ox7* functions in the cytoplasm (Fig. 4D).

### 3.8. *MdGA2ox7* overexpression caused GA-deficiency dwarfing and late flowering

Given the pivotal role of gibberellin in regulating both vegetative growth and reproductive development, the biological functions of *MdGA2ox7* were thoroughly investigated in Arabidopsis. As expected, Overexpression of *MdGA2ox7* resulted in a remarkable delay in flowering, as evident from the phenotypic analysis (Fig. 5A–C). Moreover, the plants exhibited a significant reduction in height, accompanied by shortened internode length (Fig. 5D–E). Lower levels of active GA (GA<sub>4</sub>) were recorded in the *MdGA2ox7*-overexpressing lines compared to the WT (Fig. 6B). Recognizing that the effect of GA on floral induction is particularly pronounced under short-day conditions, exogenous GA (GA<sub>3</sub>) spray treatment was performed under such conditions to verify that the delayed flowering phenotype observed in the *MdGA2ox7*-overexpressing lines was indeed due to GA deficiency. Remarkably, as demonstrated in Fig. 6 A and C, GA<sub>3</sub> supplementation can effectively restore the flowering phenotype.

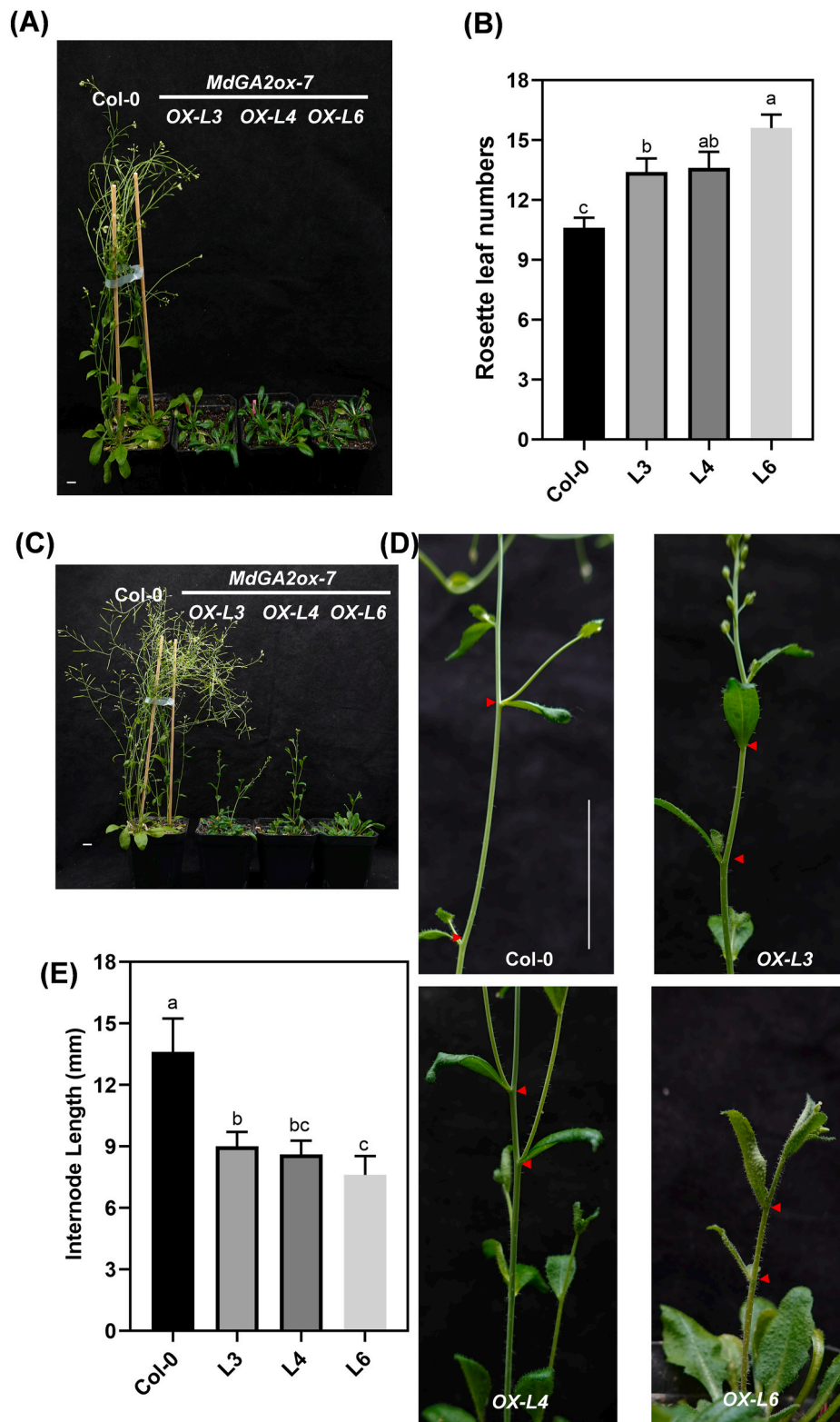


**Fig. 5.** Growth and development phenotype of *MdGA2ox7* transgenic Arabidopsis. (A) and (C) Flowering phenotypes of *MdGA2ox7* transgenic Arabidopsis. (B) Number of rosette leaves at the time of bolting. (D) and (E) Internode lengths of transgenic Arabidopsis. Bar = 1 cm. Each value represents the means  $\pm$  SD (n = 10).

### 3.9. *MdGA2ox7* worked collaboratively with MT to alleviate salt and cold damage in Arabidopsis

The *MdGA2ox7*-overexpressing lines exhibited a superior survival rate compared to the WT following freezing injury (Fig. 7 A and B). Additionally, under salt treatment, the cotyledon greening in

*MdGA2ox7*-overexpressing lines was distinguishable from that observed in the WT plants (Fig. 7 C and D). Stress can inflict damage on the photosynthetic system of plants and elevate the levels of ROS. Under salt stress, the photosynthetic system of all lines was damaged to some extent; however, the *MdGA2ox7*-overexpressing lines exhibited a lower degree of injury (Fig. 8A–C). Furthermore, the application of MT can

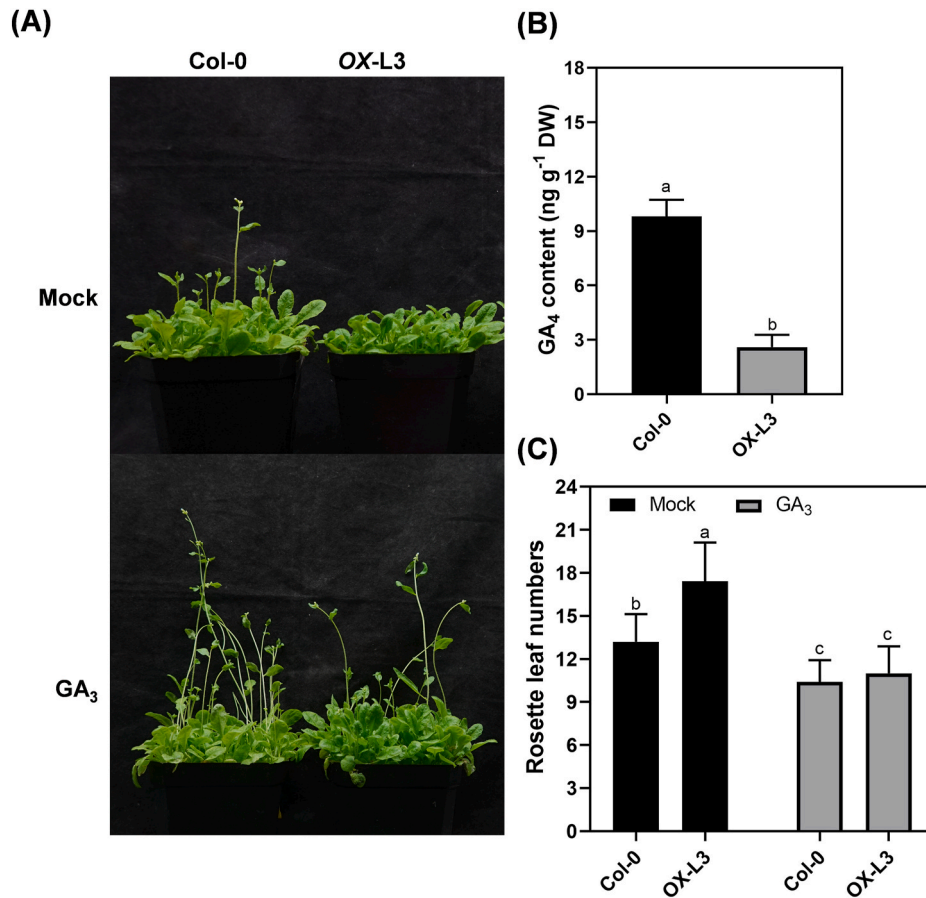


**Fig. 6.** Flowering phenotype of Arabidopsis treated with GA<sub>3</sub> spray. (A) Flowering phenotype under short-day conditions, with or without GA<sub>3</sub> treatment. (B) Number of rosette leaves at the time of bolting. (C) The active gibberellin GA<sub>4</sub> content.

restore the function of the photosynthetic system. The *MdGA2ox7*-overexpressing lines accumulated lower levels of ROS, as demonstrated by NBT staining and ROS content determination (Fig. 8D–F), suggesting that *MdGA2ox7* can mitigate ROS production triggered by salt stress. Similarly, *MdGA2ox7* overexpression also attenuated photosynthetic damage and reduced ROS accumulation under cold stress (Fig. 8A–C). Moreover, this relief effect of *MdGA2ox7* was further enhanced with the application of MT (Fig. 8). These findings suggest that *MdGA2ox7* collaborates with MT to confer resilience against cold and salt stress in plants.

### 3.10. *MdGA2ox7* alleviated salt and cold stress in apple

The function of *MdGA2ox7* under abiotic stress was further characterized in apple callus (Fig. 9). No significant differences in calli size or fresh weight were observed between the EV (empty vector) and *MdGA2ox7* transgenic lines under the control conditions. However, upon exposure to cold stress, a marked inhibition of growth was observed in the EV lines. Conversely, the *MdGA2ox7*-overexpressing line exhibited a significantly attenuated inhibitory effect, while the *MdGA2ox7*-antisense line displayed a heightened sensitivity to cold stress. These findings strongly indicate that *MdGA2ox7* positively modulates cold tolerance in apples. Similarly, under salt stress conditions, the *MdGA2ox7* overexpression line displayed a significantly alleviated growth inhibition compared to the EV line. Conversely, the inhibitory effect was exacerbated in the *MdGA2ox7*-antisense line. Therefore, *MdGA2ox7* also plays a pivotal role in enhancing tolerance to salt stress. Furthermore, the inclusion of MT in the medium can further enhance the salt and cold stress tolerance of transgenic lines (Fig. 9), hinting at a potential synergistic interaction between *MdGA2ox7* and

MT in conferring stress mitigation in apples.

### 3.11. *MdGA2ox7* promoted anthocyanin accumulation in apple

A stable transformation experiment revealed that overexpression of *MdGA2ox7* led to a significant enhancement of anthocyanin pigmentation accumulation in transgenic apple callus (Fig. 10 A and B). Consistently, the genes involved in anthocyanin synthesis were noticeably activated in the overexpressed lines (Fig. 10 C). On the contrary, transcriptional repression of *MdGA2ox7* suppressed the expression of anthocyanin synthesis genes and resulted in a decrease in anthocyanin content (Fig. 10 C).

## 4. Discussion

GA played a role in shaping plant stature, profoundly impacting agriculture and emerging as a crucial component of the 'Green Revolution'. The intricate homeostasis and signal transduction mechanisms of active gibberellin are orchestrated by a variety of enzymes and transcription factors. Notably, enzymes like GA2-oxidase can inactivate GA ultimately leading to a GA-deficient phenotype (Li et al., 2020). In horticultural plants, the encoding gene of GA2-oxidase was identified through comprehensive genome annotation. Nevertheless, the functional characterization of these genes remains limited. In this study, we identified 17 GA2ox members in the apple genome through a homologous comparison search, using Arabidopsis GA2ox as a search query (Table 1). The higher number of members may be because apple (742.3 Mb) has a larger complex genomic structure compared to grape (416.1 Mb) and peach (228.82 Mb). The *MdGA2ox* genes can be categorized into two major classes and four minor groups, based on the conserved

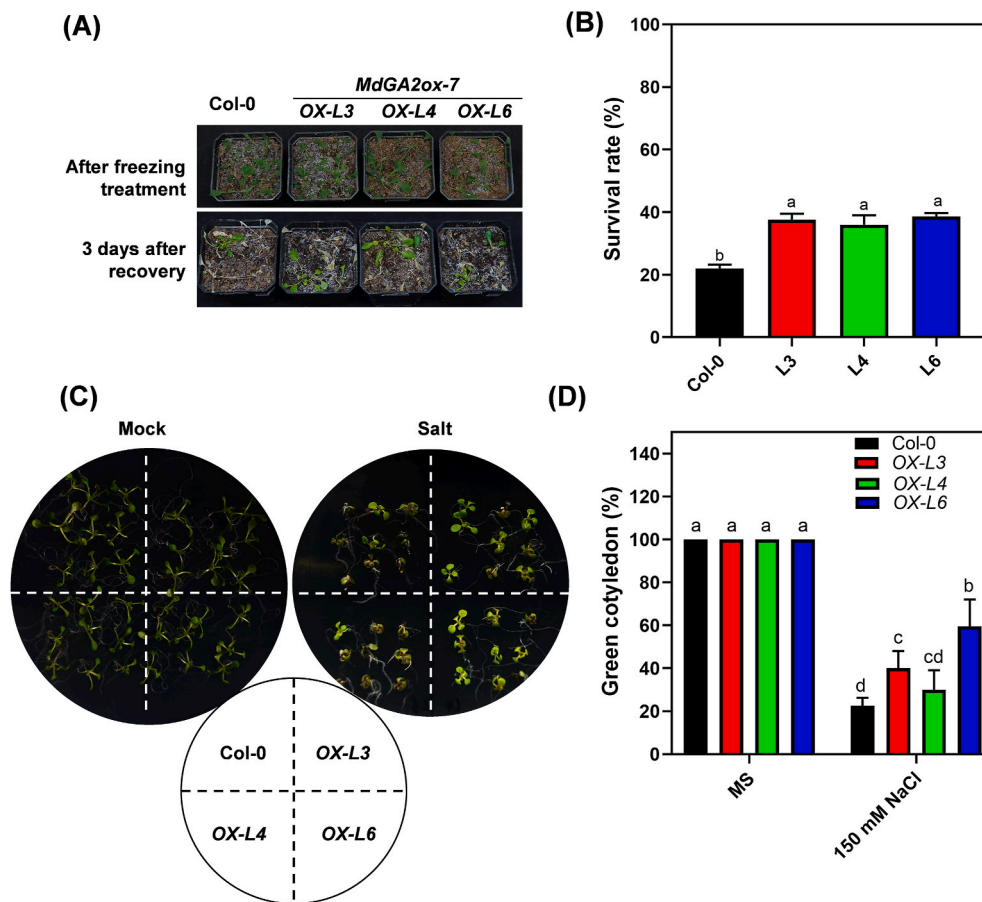


**Fig. 7.** Phenotype of *MdGA2ox7* transgenic *Arabidopsis* under freezing and salt stress. (A) Phenotypic comparison under freezing stress. (B) Survival rate under freezing stress. (C) Phenotypic comparison under salt stress. (D) Cotyledon greening ratio under salt stress.

motif and the substrate forms they can catalyze (Fig. 1). Furthermore, the expansion of *MdGA2ox*'s membership may be due to gene duplication, as suggested by the collinearity analysis (Supplementary Fig. S1A). Homologous genes arising from duplication often exhibit similarities in gene structure and expression patterns, such as *MdGA2ox5/9* and *MdGA2ox13/15* gene pairs (Figs. 1B and 2), which is the reason for maintaining the stability of gene function. However, during gene family expansion, fragment insertion/deletion events can lead to changes in gene structure (Fig. 1B), despite maintaining conserved motifs (Fig. 1C) and expression patterns (Fig. 2A). Additionally, diversity can also manifest in the promoter regions (such as variations in *cis*-regulatory elements, Supplementary Fig. S2), which may lead to their ability to be recognized by specific transcription factors and respond to specific environmental signals, as reported previously (Zhang et al., 2018).

The high transcription level of *MdGA2ox7*, a member of Group II C<sub>19</sub>-GA2ox-II, across multiple tissues (Figs. 2 and 3A) prompted a deeper exploration of its biological function. Subcellular localization results revealed that *MdGA2ox7* was located in the cytoplasm (Fig. 4). Remarkably, all of the apple *MdGA2ox* members were predicted to reside in the cytoplasm (Supplementary Table S1). The protein sequence and structure analysis of *MdGA2ox7* revealed that the GA<sub>4</sub> binding site was conserved with the *OsGA2ox3* homolog (Fig. 4C), which has been demonstrated to lead to a decrease in endogenous GA<sub>4</sub> level and a dwarfing phenotype (Guo et al., 2013). Consistent with these findings, the content of active gibberellin GA<sub>4</sub> was significantly reduced in the *MdGA2ox7* overexpression lines (Fig. 6B). As a concomitant phenotype, the transgenic plants exhibited reduced plant height and delayed flowering traits, which could be reversed by the application of exogenous GA<sub>3</sub> (Figs. 5 and 9). Similar phenotypic alterations have been observed in other plants where *GA2ox* expression levels were modulated. For

instance, overexpression of the *TaGA2ox-A9* led to a reduction of bioactive GA, resulting in decreased plant height (*Triticum aestivum*) (Tian et al., 2022). Conversely, reduction of *GA2ox* transcript by virus-induced gene silencing (VIGS) resulted in a significant stem elongation in *Petunia hybrida* 'Fantasy Blue' (Gargul et al., 2015). In plum (*Prunus salicina*), *PslGA2ox* has been explored as a potential tool for developing size-controlling rootstocks (El-Sharkawy et al., 2012). Moreover, the *GA2ox* gene from the *Rosaceae* family also showed a similar function. For instance, *PavGA2ox-2L* from sweet cherry (*Prunus avium*) (Liu et al., 2022), and three *GA2ox* from peach (*Prunus persica*) (Cheng et al., 2021) have been shown to promote dwarf and delay flowering, indicating that the regulatory roles of *GA2ox* in plant growth and development are extensively conserved across different species. Furthermore, *GA2ox* has been implicated in affecting fertilization processes (Lange et al., 2020) and fruit set (Serrani et al., 2007), highlighting its diverse functions in plant reproduction. Consequently, there remains a need for more comprehensive investigations into the specific functions of *MdGA2ox7* functions in regulating plant development.

Salt and cold stress pose significant threats to China's apple industry. In response to these stressors, apple seedlings showed symptoms of wilting and growth inhibition, accompanied by a surge in ROS levels (Fig. 3C–E). Notably, the promoter region of *MdGA2ox* harbors a significant number of stress response-related CRE (Supplementary Fig. S2). Intriguingly, the activity of *MdGA2ox7* promoter was markedly upregulated in response to both cold and salt treatment (Fig. 3B). Similar trends have been observed in maize (*Zea mays*), where *GA2ox* gene expression responds to diverse stress conditions, including salt, cold, and drought (Li et al., 2021). However, the specific gene function in stress response remains elusive. Our findings have clarified the role of *MdGA2ox7* in stress response. Overexpression of *MdGA2ox7* conferred

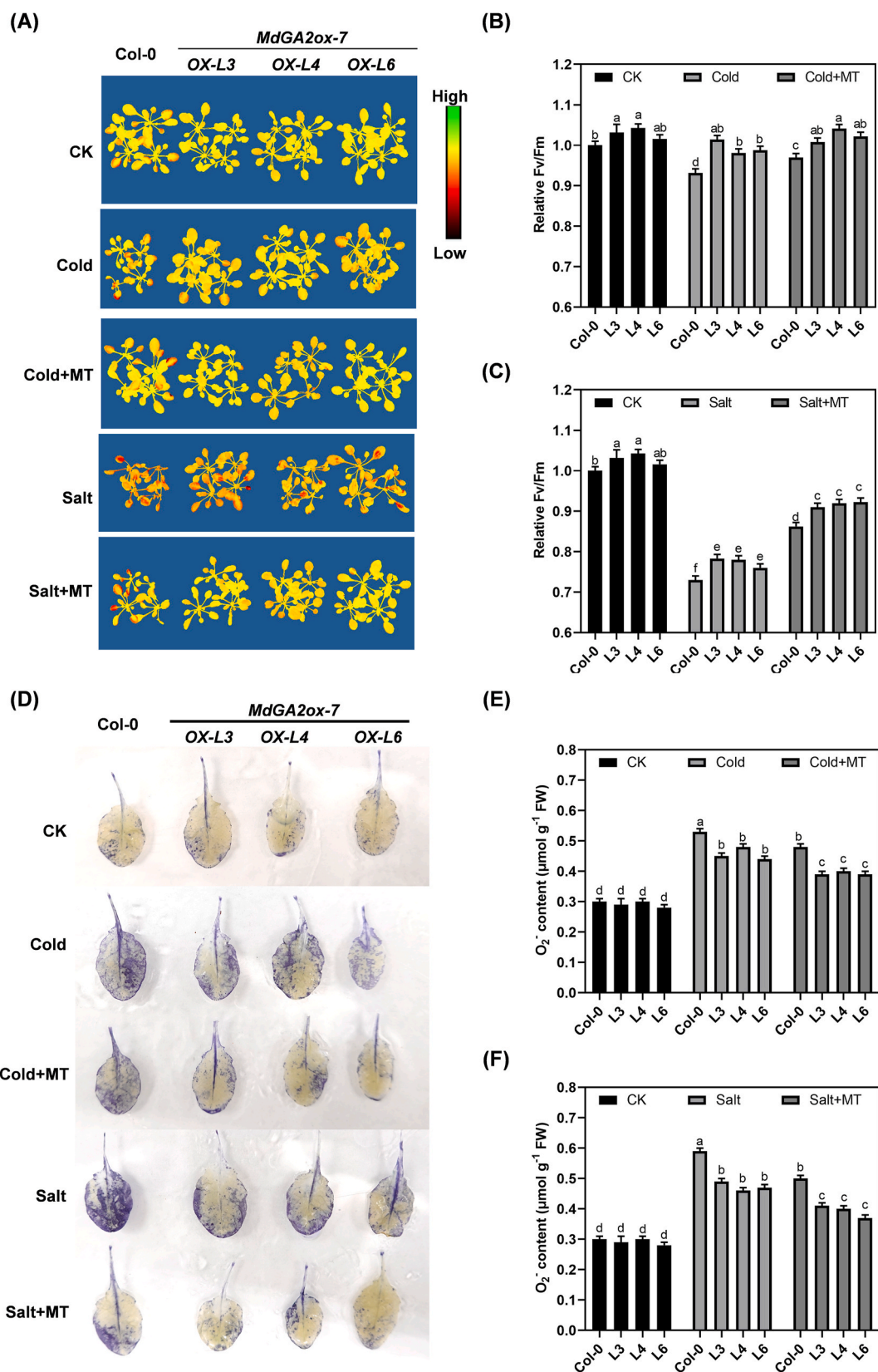


**Fig. 8.** Characterization of damage in *MdGA2ox7* transgenic *Arabidopsis* under cold and salt stress, supplemented with MT. (A)–(C) represented changes in photosynthetic parameters. (A) showed the chlorophyll fluorescence imaging (Fv/Fm) of wild-type (Col-0) and *MdGA2ox7*-overexpressing (*MdGA2ox7*-OX) transgenic lines under cold and salt stress, with or without MT supplementation. (B) and (C) showed the Fv/Fm ratios. (D)–(F) represented the accumulation of ROS under cold and salt stress, with or without MT supplementation. (D) showed the  $O_2^-$  accumulation in the leaves by histochemical staining with NBT. (E) and (F) Quantitative measurement of ROS concentration in *Arabidopsis* leaves.

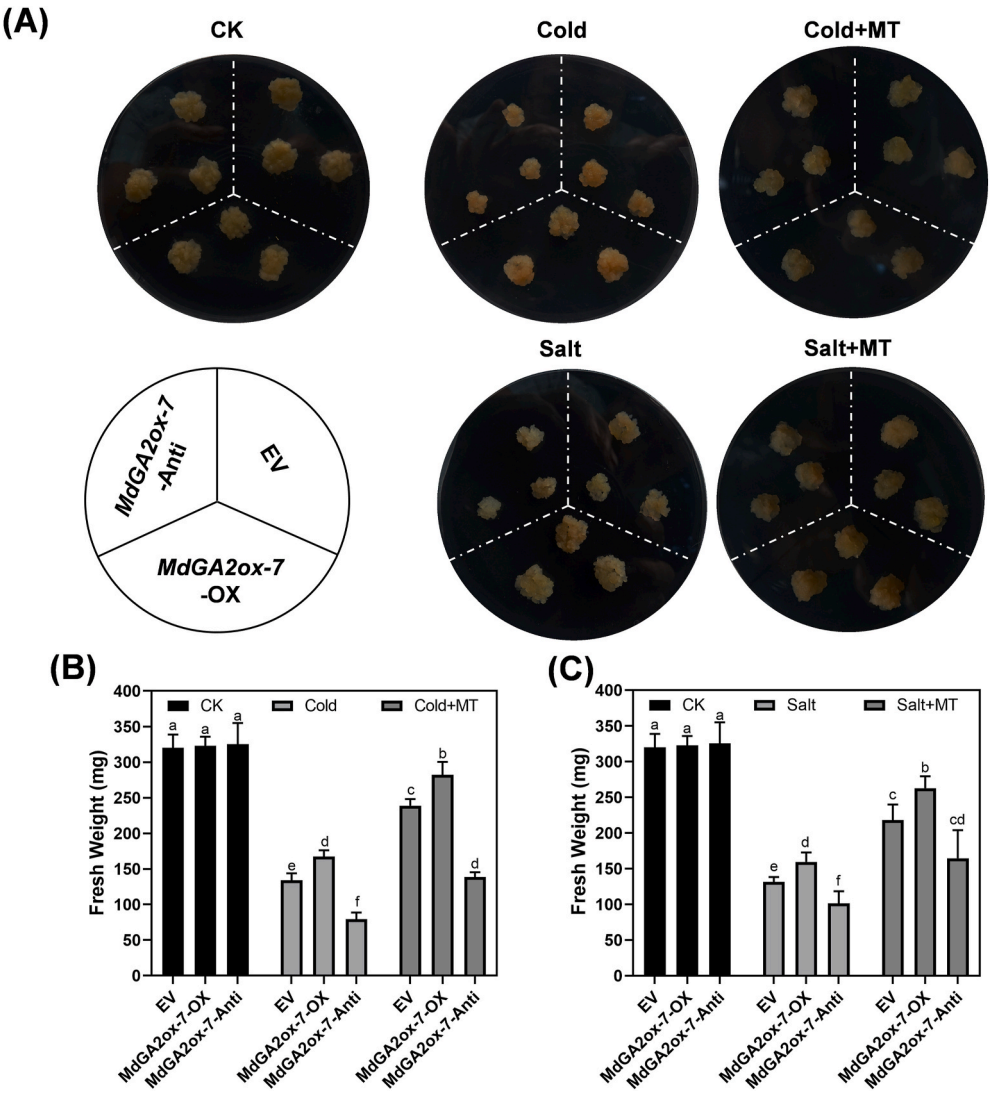


**Fig. 9.** Characterization of damage in *MdGA2ox7* transgenic apple calli under cold and salt stress, supplemented with MT. (A) Phenotypes of transgenic apple calli (EV, empty vector; *MdGA2ox7-OX*, *MdGA2ox7* overexpression; *MdGA2ox7-Anti*, *MdGA2ox7* antisense suppression) under cold and salt stress. (B) and (C) presented the fresh weight of transgenic apple calli after cold and salt treatment with or without MT supplementation, respectively.

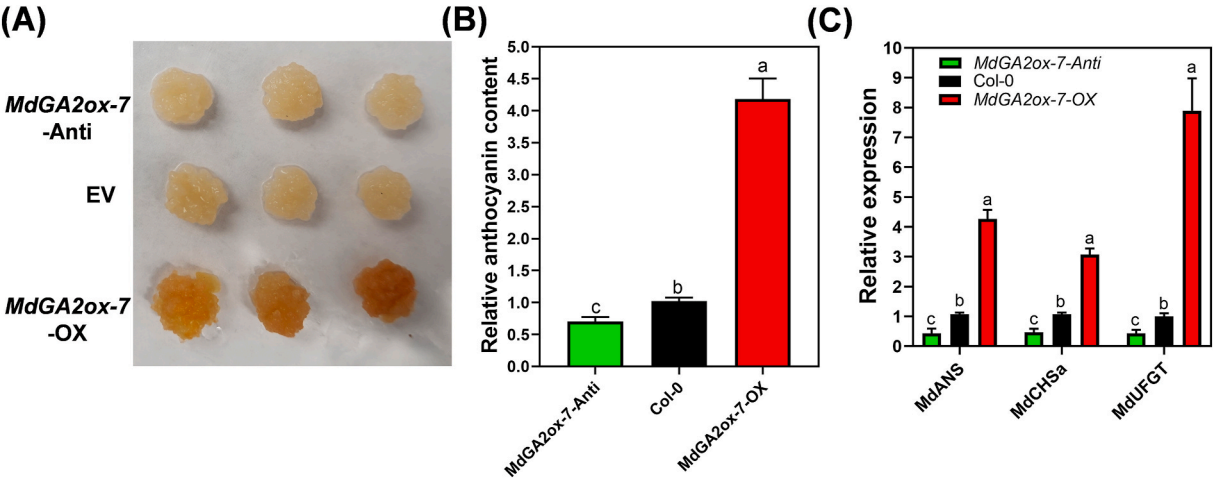


**Fig. 10.** Functional analysis of *MdGA2ox7* in anthocyanin biosynthesis. (A) Twenty-day-old transgenic apple calli masses incubated under constant light at 23 °C. (B) Quantification of anthocyanin content. (C) Expression levels of anthocyanin synthesis gene. The anthocyanin content and gene expression level in EV callus were set to 1.

resistance to cold and salt stress in both apple and Arabidopsis (Figs. 7–9), marking the first report that *GA2ox* regulating stress responses in apple. It reported that sometimes it is best to limit growth under stressful conditions, and survival is enhanced by reduced GA synthesis under salt stress (Yu et al., 2020). Furthermore, the application of GA in chrysanthemums aggravated the harm caused by low temperature (Yang et al., 2014), indicating that high GA levels are not favorable for plants survival in adverse environments. Consequently, overexpressing *MdGA2ox7* results in decreased levels of active GA, thereby enhancing the plant's tolerance to salt and cold stress. Additionally, the emerging hormone MT has demonstrated its capacity to enhance various stress tolerance in horticultural crops. Our current research reveals that the integration of MT further alleviated stress damage in *MdGA2ox7* overexpressing lines, both in Arabidopsis and apple (Figs. 7–9). This observation suggests a synergistic effect between these two factors in response to adverse environmental conditions. Additionally, crosstalk between microRNAs and GA signaling has been reported in various plant species, with microRNAs playing a pivotal role in GA-related gene expression and stress response (Yu and Wang, 2020). Therefore, the relationship between *MdGA2ox7* and microRNAs merits further exploration. Given its potential, *MdGA2ox7* could serve as an ideal candidate gene for developing rootstocks that regulate tree size and confer stress tolerance to grafted trees.

Gibberellin has been implicated in secondary metabolic processes in plants, particularly in anthocyanin accumulation (Li and Ahammed, 2023). Our current study revealed that *MdGAox7* was significantly activated during the transition from green to red in apple under light conditions after unbagging (Fig. 2C). After bag removal, the green-skinned apple develops red pigmentation with significantly increased anthocyanin content (Ma et al., 2019). Notably, the abundant presence of light-responsive *CRE* on the *MdGA2ox7* promoter indicates its involvement in photoinduced anthocyanin accumulation (Supplementary Fig. S2). Furthermore, *MdGAox7* enhanced anthocyanin accumulation and up-regulated the expression levels of several anthocyanin synthesis genes (Fig. 10). Parallel findings in pear fruit peel, where *PbGA2ox8* induces anthocyanin accumulation, and the role of DELLA proteins in promoting anthocyanin biosynthesis (Xie et al., 2016; Zhai et al., 2019), suggest a conserved function of endogenous gibberellin levels and signaling pathways in regulating anthocyanin accumulation. Given the protective role of anthocyanin against abiotic stress in plants, it is plausible that *MdGA2ox7*'s improvement in cold and salt tolerance is attributed to its stimulatory effect on anthocyanin accumulation.

## 5. Conclusion

In this study, we discovered that the overexpression of *MdGA2ox7* can effectively reduce the content of active GA, leading to phenotypic manifestations such as delayed flowering and shortened internode. *MdGA2ox7* is up-regulated in response to cold and salt treatment and cooperates with MT to regulate stress tolerance in both apple and Arabidopsis. *MdGA2ox7* promotes anthocyanin accumulation and enhances the expression of genes involved in anthocyanin synthesis. These findings lay a solid foundation for future research on the functional roles of *GA2ox* genes and provide candidate genes for molecular breeding aimed at improving various horticultural traits, including flower development, dwarfism, and anthocyanin-related stress resistance.

## CCRediT authorship contribution statement

**Rui Yan:** Methodology, Investigation, Formal analysis, Data curation. **Tianle Zhang:** Visualization, Validation, Software, Methodology. **Yuan Wang:** Writing – original draft, Resources, Formal analysis, Conceptualization. **Wenxiu Wang:** Visualization, Validation. **Rahat Sharif:** Writing – review & editing, Software. **Jiale Liu:** Software, Methodology, Investigation, Formal analysis, Data curation. **Qinglong Dong:** Supervision, Investigation, Conceptualization. **Haoan Luan:**

Resources, Formal analysis, Data curation. **Xuemei Zhang:** Supervision, Funding acquisition, Data curation. **Han Li:** Validation, Resources, Data curation. **Suping Guo:** Supervision, Conceptualization. **Guohui Qi:** Writing – original draft, Visualization, Validation, Supervision, Conceptualization. **Peng Jia:** Writing – review & editing, Writing – original draft, Funding acquisition, Conceptualization.

## Declaration of competing interest

The authors declare that they have no known competing financial interests or personal relationships that could have appeared to influence the work reported in this paper.

## Data availability

Data will be made available on request.

## Acknowledgments

This work was supported by The Natural Science Research Project of Colleges and Universities in Hebei Province (QN2023191), The Hebei Natural Science Foundation (C2022204016), The Special scientific research project for the introduction of talents in Hebei Agricultural University (YJ2021026), and The Hebei Agriculture Research System (HBCT2024150206).

## Appendix A. Supplementary data

Supplementary data to this article can be found online at <https://doi.org/10.1016/j.plaphy.2024.108707>.

## References

- An, J.P., Zhang, X.W., Li, H.L., Wang, D.R., You, C.X., Han, Y., 2023. The E3 ubiquitin ligases SINA1 and SINA2 integrate with the protein kinase CIPK20 to regulate the stability of RGL2a, a positive regulator of anthocyanin biosynthesis. *New Phytol.* 239, 1332–1352.
- Bajwa, V.S., Shukla, M.R., Sherif, S.M., Murch, S.J., Saxena, P.K., 2014. Role of melatonin in alleviating cold stress in *Arabidopsis thaliana*. *J. Pineal Res.* 56, 238–245.
- Cheng, J., Ma, J., Zheng, X., Lv, H., Zhang, M., Tan, B., Ye, X., Wang, W., Zhang, L., Li, Z., Li, J., Feng, J., 2021. Functional analysis of the *gibberellin 2-oxidase* gene family in peach. *Front. Plant Sci.* 12.
- El-Sharkawy, I., El Kayal, W., Prasath, D., Fernández, H., Bouzayen, M., Svircev, A.M., Jayasankar, S., 2012. Identification and genetic characterization of a gibberellin 2-oxidase gene that controls tree stature and reproductive growth in plum. *J. Exp. Bot.* 63, 1225–1239.
- Gargul, J.M., Mibus, H., Serek, M., 2015. Phenotypic effects and the quantification of transcript abundance in *Petunia hybrida* 'Fantasy Blue' with virus-induced *GA2ox* gene silencing. *Sci. Hortic.* 197, 226–229.
- Guo, X., Hou, X., Fang, J., Wei, P., Xu, B., Chen, M., Feng, Y., Chu, C., 2013. The rice *GERMINATION DEFECTIVE 1*, encoding a B3 domain transcriptional repressor, regulates seed germination and seedling development by integrating GA and carbohydrate metabolism. *Plant J.* 75, 403–416.
- Hedden, P., 2020. The current status of research on gibberellin biosynthesis. *Plant Cell Physiol.* 61, 1832–1849.
- Hernández, I.G., Gomez, F.J., Cerutti, S., Arana, M.V., Silva, M.F., 2015. Melatonin in *Arabidopsis thaliana* acts as plant growth regulator at low concentrations and preserves seed viability at high concentrations. *Plant Physiol. Biochem.* 94, 191–196.
- Jia, P., Wang, Y., Sharif, R., Ren, X., Qi, G., 2023. *MdIPT1*, an adenylate isopentenyltransferase coding gene from *Malus domestica*, is involved in branching and flowering regulation. *Plant Sci.* 333, 111730.
- Jia, P., Xing, L., Zhang, C., Zhang, D., Ma, J., Zhao, C., Han, M., Ren, X., An, N., 2021. MdKNOX19, a class II knotted-like transcription factor of apple, plays roles in ABA signalling/sensitivity by targeting *ABI5* during organ development. *Plant Sci.* 302, 110701.
- Lange, T., Krämer, C., Pimenta Lange, M.J., 2020. The class III gibberellin 2-oxidases AtGA2ox9 and AtGA2ox10 contribute to cold stress tolerance and fertility. *Plant Physiol.* 184, 478–486.
- Li, C., Zheng, L., Wang, X., Hu, Z., Zheng, Y., Chen, Q., Hao, X., Xiao, X., Wang, X., Wang, G., Zhang, Y., 2019a. Comprehensive expression analysis of Arabidopsis *GA2-oxidase* genes and their functional insights. *Plant Sci.* 285, 1–13.
- Li, R., Sun, S., Wang, H., Wang, K., Yu, H., Zhou, Z., Xin, P., Chu, J., Zhao, T., Wang, H., Li, J., Cui, X., 2020. *FIS1* encodes a GA2-oxidase that regulates fruit firmness in tomato. *Nat. Commun.* 11, 5844.

- Li, Y., Shan, X., Jiang, Z., Zhao, L., Jin, F., 2021. Genome-wide identification and expression analysis of the GA2ox gene family in maize (*Zea mays* L.) under various abiotic stress conditions. *Plant Physiol. Biochem.* 166, 621–633.
- Li, Y., Zhang, D., An, N., Fan, S., Zuo, X., Zhang, X., Zhang, L., Gao, C., Han, M., Xing, L., 2019b. Transcriptomic analysis reveals the regulatory module of apple (*Malus x domestica*) floral transition in response to 6-BA. *BMC Plant Biol.* 19, 93.
- Li, Z., Ahammed, G.J., 2023. Hormonal regulation of anthocyanin biosynthesis for improved stress tolerance in plants. *Plant Physiol. Biochem.* 201, 107835.
- Liu, J., Zhai, R., Liu, F., Zhao, Y., Wang, H., Liu, L., Yang, C., Wang, Z., Ma, F., Xu, L., 2018. Melatonin induces parthenocarp by regulating genes in gibberellin pathways of 'starkrimson' pear (*Pyrus communis* L.). *Front. Plant Sci.* 9, 946.
- Liu, X., Wang, J., Sabir, I.A., Sun, W., Wang, L., Xu, Y., Zhang, N., Liu, H., Jiu, S., Liu, L., Zhang, C., 2022. PavGA2ox-2L inhibits the plant growth and development interacting with PavDWARF in sweet cherry (*Prunus avium* L.). *Plant Physiol. Biochem.* 186, 299–309.
- Lo, S.-F., Yang, S.-Y., Chen, K.-T., Hsing, Y.-I., Zeevaert, J.A.D., Chen, L.-J., Yu, S.-M., 2008. A novel class of gibberellin 2-oxidases control semidwarfism, tillering, and root development in rice. *Plant Cell* 20, 2603–2618.
- Lv, Y., Pan, J., Wang, H., Reiter, R.J., Li, X., Mou, Z., Zhang, J., Yao, Z., Zhao, D., Yu, D., 2021. Melatonin inhibits seed germination by crosstalk with abscisic acid, gibberellin, and auxin in Arabidopsis. *J. Pineal Res.* 70, e12736.
- Ma, C., Liang, B., Chang, B., Yan, J., Liu, L., Wang, Y., Yang, Y., Zhao, Z., 2019. Transcriptome profiling of anthocyanin biosynthesis in the peel of 'Granny Smith' apples (*Malus domestica*) after bag removal. *BMC Genomics* 20, 353.
- Magome, H., Yamaguchi, S., Hanada, A., Kamiya, Y., Oda, K., 2008. The DDF1 transcriptional activator upregulates expression of a gibberellin-deactivating gene, GA2ox7, under high-salinity stress in Arabidopsis. *Plant J.* 56, 613–626.
- Rieu, I., Eriksson, S., Powers, S.J., Gong, F., Griffiths, J., Woolley, L., Benlloch, R., Nilsson, O., Thomas, S.G., Hedden, P., Phillips, A.L., 2008. Genetic analysis reveals that C<sub>19</sub>-GA 2-oxidation is a major gibberellin inactivation pathway in Arabidopsis. *Plant Cell* 20, 2420–2436.
- Schomburg, F.M., Bizzell, C.M., Lee, D.J., Zeevaert, J.A., Amasino, R.M., 2003. Overexpression of a novel class of gibberellin 2-oxidases decreases gibberellin levels and creates dwarf plants. *Plant Cell* 15, 151–163.
- Serrani, J.C., Sanjuán, R., Ruiz-Rivero, O., Fos, M., García-Martínez, J.L., 2007. Gibberellin regulation of fruit set and growth in tomato. *Plant Physiol.* 145, 246–257.
- Su, J., Yang, X., Shao, Y., Chen, Z., Shen, W., 2021. Molecular hydrogen-induced salinity tolerance requires melatonin signalling in Arabidopsis thaliana. *Plant Cell Environ.* 44, 476–490.
- Sun, C., Liu, L., Wang, L., Li, B., Jin, C., Lin, X., 2021. Melatonin: a master regulator of plant development and stress responses. *J. Integr. Plant Biol.* 63, 126–145.
- Takehara, S., Sakuraba, S., Mikami, B., Yoshida, H., Yoshimura, H., Itoh, A., Endo, M., Watanabe, N., Nagae, T., Matsuoka, M., Ueguchi-Tanaka, M., 2020. A common allosteric mechanism regulates homeostatic inactivation of auxin and gibberellin. *Nat. Commun.* 11, 2143.
- Tian, X., Xia, X., Xu, D., Liu, Y., Xie, L., Hassan, M.A., Song, J., Li, F., Wang, D., Zhang, Y., Hao, Y., Li, G., Chu, C., He, Z., Cao, S., 2022. Rht24b, an ancient variation of TaGA2ox-A9, reduces plant height without yield penalty in wheat. *New Phytol.* 233, 738–750.
- Wang, Y., Li, W., Xu, X., Qiu, C., Wu, T., Wei, Q., Ma, F., Han, Z., 2019. Progress of apple rootstock breeding and its use. *Hortic. Plant J.* 5, 183–191.
- Wuddineh, W.A., Mazarei, M., Zhang, J., Poovaiah, C.R., Mann, D.G., Ziebell, A., Sykes, R.W., Davis, M.F., Udvardi, M.K., Stewart Jr., C.N., 2015. Identification and overexpression of gibberellin 2-oxidase (GA2ox) in switchgrass (*Panicum virgatum* L.) for improved plant architecture and reduced biomass recalcitrance. *Plant Biotechnol. J.* 13, 636–647.
- Xie, Y., Tan, H., Ma, Z., Huang, J., 2016. DELLA proteins promote anthocyanin biosynthesis via sequestering MYBL2 and JAZ suppressors of the MYB/bHLH/WD40 complex in Arabidopsis thaliana. *Mol. Plant* 9, 711–721.
- Yang, J., Cao, Y., Zhang, N., 2020. Spectrophotometric method for superoxide anion radical detection in a visible light (400–780 nm) system. *Spectrochim. Acta Mol. Biomol. Spectrosc.* 239, 118556.
- Yang, Y., Ma, C., Xu, Y., Wei, Q., Imtiaz, M., Lan, H., Gao, S., Cheng, L., Wang, M., Fei, Z., Hong, B., Gao, J., 2014. A zinc finger protein regulates flowering time and abiotic stress tolerance in Chrysanthemum by modulating gibberellin biosynthesis. *Plant Cell* 26, 2038–2054.
- Yu, S., Wang, J.W., 2020. The crosstalk between MicroRNAs and gibberellin signaling in plants. *Plant Cell Physiol.* 61, 1880–1890.
- Yu, Z., Duan, X., Luo, L., Dai, S., Ding, Z., Xia, G., 2020. How plant hormones mediate salt stress responses. *Trends Plant Sci.* 25, 1117–1130.
- Zaid, A., Wani, S.H., 2019. Reactive oxygen species generation, scavenging and signaling in plant defense responses. In: Jogaiah, S., Abdelrahman, M. (Eds.), *Bioactive Molecules in Plant Defense: Signaling in Growth and Stress*. Springer International Publishing, Cham, pp. 111–132.
- Zhai, R., Wang, Z., Yang, C., Lin-Wang, K., Espley, R., Liu, J., Li, X., Wu, Z., Li, P., Guan, Q., Ma, F., Xu, L., 2019. PbGA2ox8 induces vascular-related anthocyanin accumulation and contributes to red stripe formation on pear fruit. *Hortic. Res.* 6, 137.
- Zhang, Q., Ma, C., Zhang, Y., Gu, Z., Li, W., Duan, X., Wang, S., Hao, L., Wang, Y., Wang, S., Li, T., 2018. A single-nucleotide polymorphism in the promoter of a hairpin RNA contributes to Alternaria alternata leaf spot resistance in apple (*Malus x domestica*). *Plant Cell* 30, 1924–1942.